SECTION 3

EXPERIMENTAL STUDY OF RETROFITTED R/C MODEL

3.1 Introduction

In Section 2, the local and global seismic concerns for and expected damage in typical GLD R/C frame buildings were discussed and verified in a previous experimental study (Bracci et al., 1992b). Based on these concerns and the expected damage for such buildings and the previous experimental damage, three seismic retrofit methods were suggested and analytically verified for the 1:3 scale R/C frame model building.

In this section, one of the suggested retrofit techniques is selected to repair and upgrade the 1:3 scale GLD R/C frame model building for an additional experimental shaking table study. Retrofit construction is described and performed on the model. The shaking table testing program for the retrofitted model, along with induced base motions, is presented. The initial dynamic characteristics of the retrofitted model are also identified from an experimental white noise shaking table excitation.

3.2 Selection of Retrofit Method for Experimental Study

It was previously shown that several of the chosen retrofit methods provide adequate control of the story drifts, shears, and damage of the structural system in event of a future strong ground motion. For a prototype structure, the selected retrofit technique would obviously depend on a number of factors such as: costs; amount of time the building (or sections) would remain closed; and the design earthquake zone, etc. However, for the model, other factors had to be considered for determining the retrofit method: the availability of scaled retrofit material (masonry blocks); maintaining proper instrumentation of the model for the experiment (ie. custom made load cells); and construction equipment required for retrofit.

In view of the above considerations, the improved concrete jacketing alternative of the critical interior columns was selected to retrofit the model structure. Although the retrofit of all columns was shown to provide somewhat better control of the inter-story drifts, a minimal retrofit of only the interior columns provides adequate seismic performance, especially for low to moderate

seismicity zones. It was previously shown that the global structural response is adequately controlled with the discontinued reinforcement at the base. To avoid any additional foundation loading, the added reinforcement in the jacketed zone is intentionally discontinued at the rigid base. Fig. 3-1 shows some of the construction stages in the retrofit of the model. The amount of work and structural disturbance is minimal. The completed retrofitted model with the required additional weights for mass similitude are shown on the shaking table in Fig. 3-1c.

3.3 Testing Schedule of Retrofitted Model

Table 3-1 shows the shaking table testing program for the retrofitted model structure. For comparison purposes, the two ground motions are selected using the Taft N21E accelerogram scaled to 0.20 g and 0.30 g, respectively in order to simulate moderate and severe earthquakes. A series of compensated white noise excitations are used before and after every earthquake test for the identification of prevailing dynamic characteristics.

TABLE 3-1 Shaking Table Testing Sequence for the Retrofitted Model

Test #	Date	Test Label	Test Description	Purpose
1	1/28/92	WHNR_B	Compensated White Noise, PGA 0.024 g	Identification
2	1/29/92	WHNR_C	Compensated White Noise, PGA 0.024 g	Identification
3	1/29/92	TFTR_20	Taft N21E, PGA 0.20 g	Moderate Earthquake, Inelastic Response
4	1/29/92	WHNR_D	Compensated White Noise, PGA 0.024 g	Identification
5	1/29/92	TFTR_30	Taft N21E, PGA 0.30 g	Severe Earthquake, Inelastic Response
6	1/29/92	WHNR_E	Compensated White Noise, PGA 0.024 g	Identification

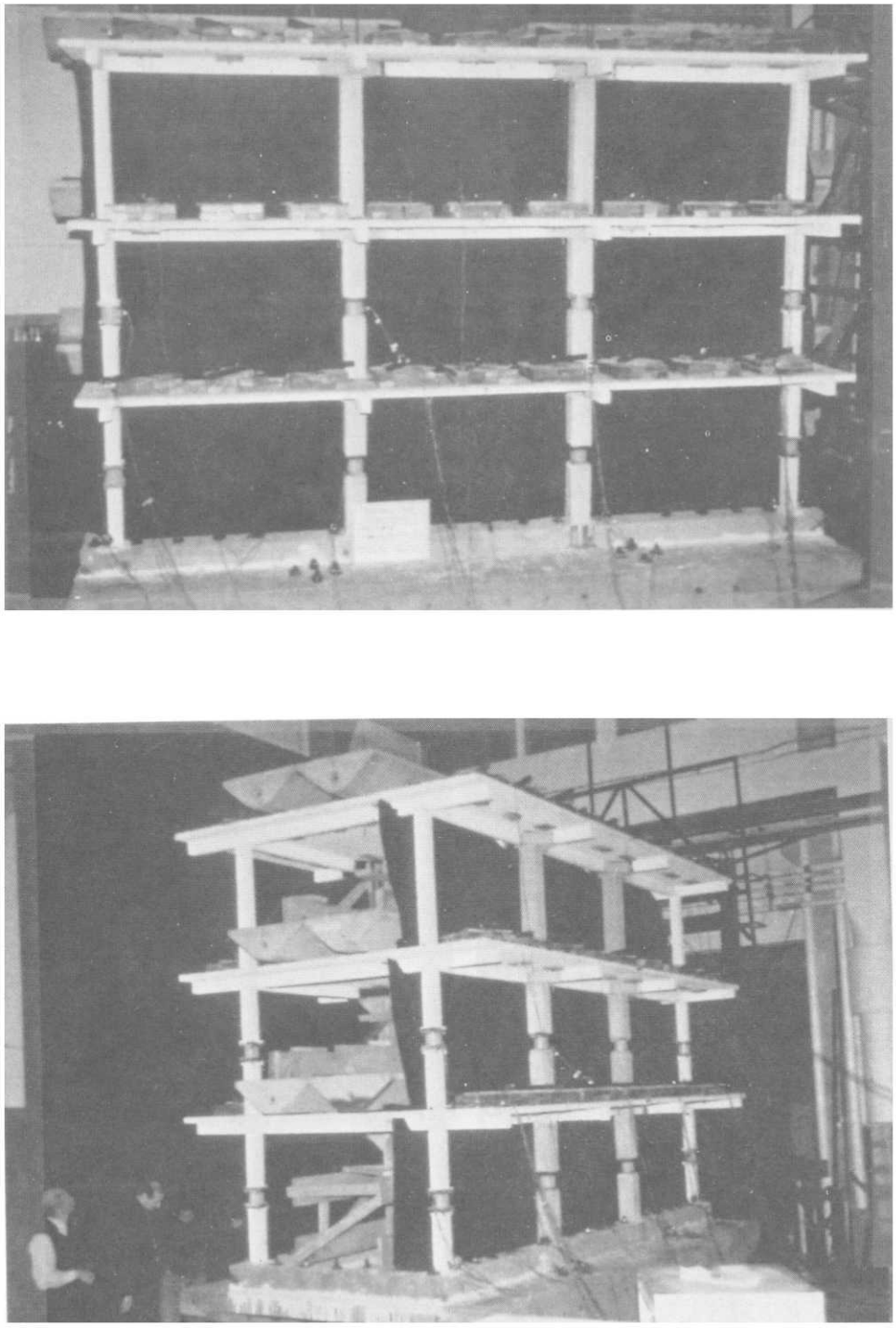

FIG. 3-1a Stages in the Improved Concrete Jacketing Retrofit of the Model.

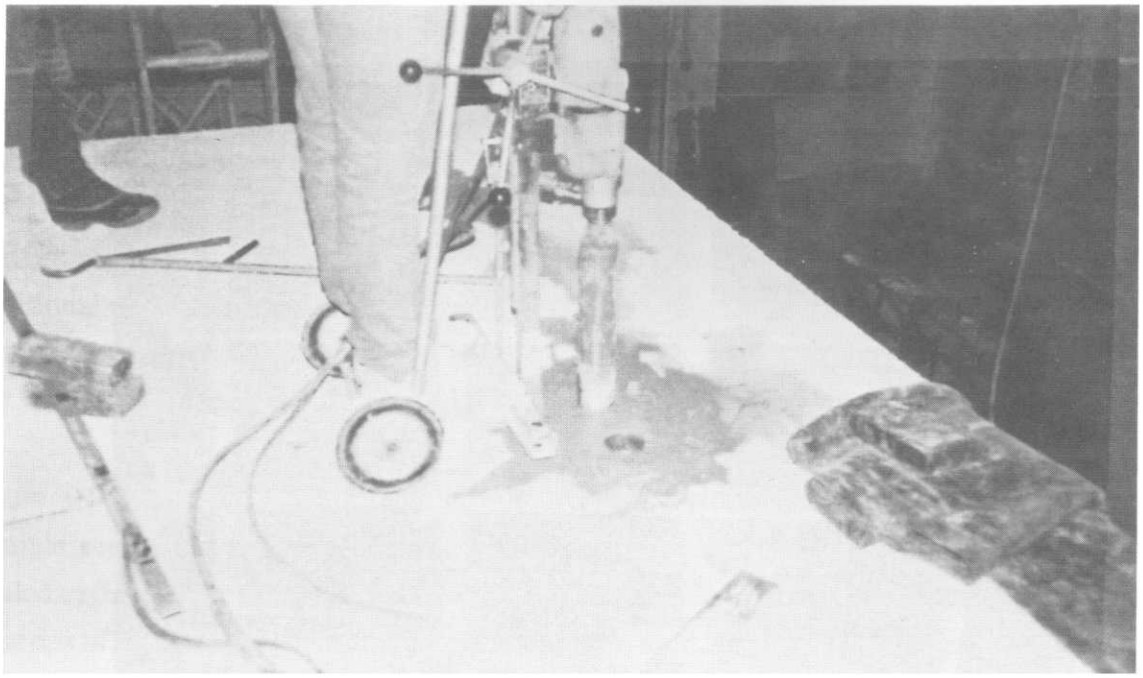

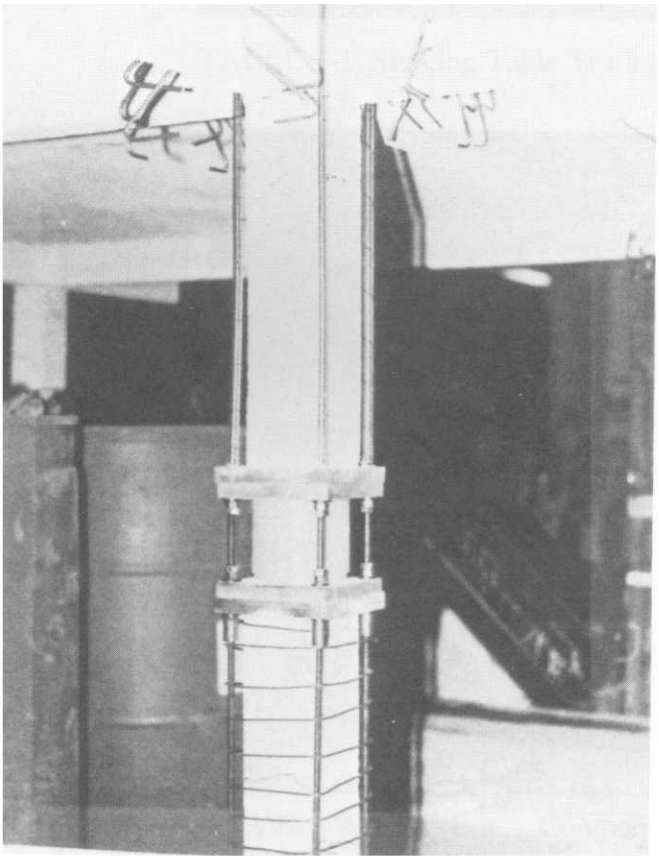

FIG. 3-1b Stages in the Improved Concrete Jacketing Retrofit of the Model (cont.)

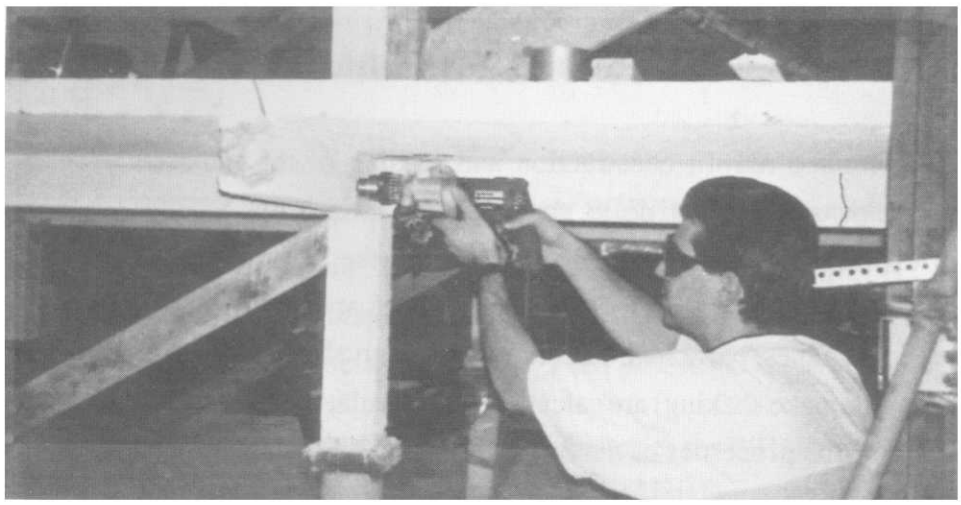

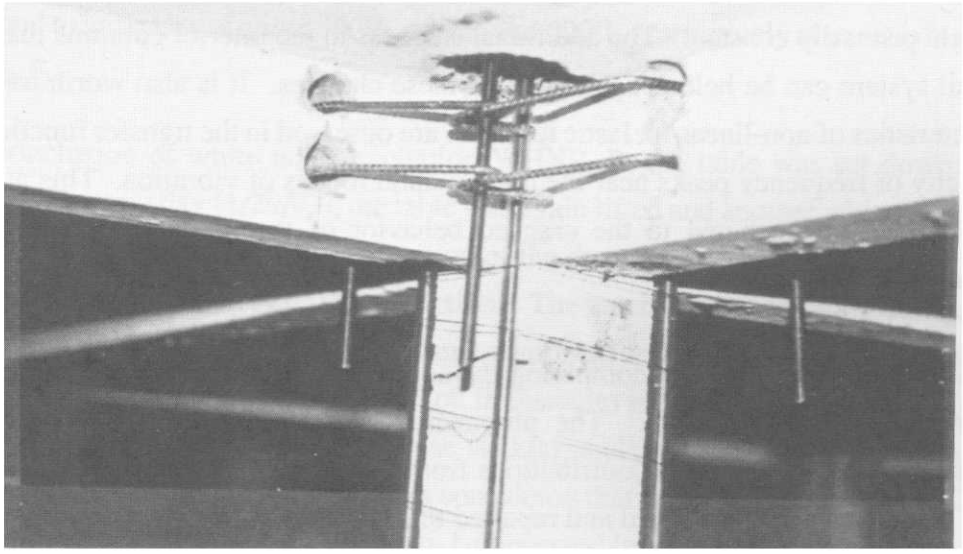

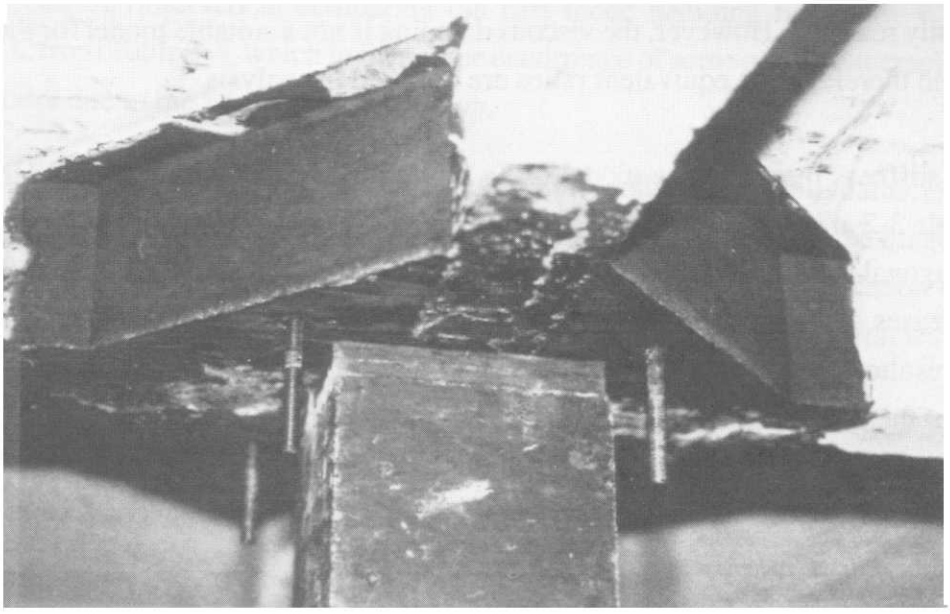

FIG. 3-1c Stages in the Improved Concrete Jacketing Retrofit of the Model (cont'd)

3.4 Dynamic Characteristics of Retrofitted Model - Before Earthquake Shaking

Following the complete retrofit construction and loading of the required weights for mass similitude, a compensated white noise shaking table excitation, WHNR_B, was used for identification of the initial dynamic characteristics of the retrofitted model. The resulting smoothed transfer functions for each floor of the model are shown in Fig. 3-2. The natural frequencies, modal shapes, participation factors, and equivalent viscous damping factors after retrofit (before earthquake shaking) are calculated and tabulated in Table 3-2. It can be observed from comparison to the properties of the original structure that the modal frequencies increase approximately 130%, 150%, and 210%, respectively due to the retrofit. Variations in the modal shapes can be detected before (WHN_F) and after (WHNR_B) retrofit, while the participation factors remain primarily constant. The additional stiffness in the interior columns that change the structural system can be held accountable for these changes. It is also worth noting that some characteristics of non-linear/inelastic response are observed in the transfer functions from the multiplicity of frequency peaks near the main/natural modes of vibration. This non-linear response is primarily attributed to the cracked behavior of the structure, particularly the unretrofitted members.

A large change can be observed in comparing the equivalent viscous damping factors before and after retrofit from Table 3-2. The unretrofitted model experienced large inelastic deformations and had considerable contributions from hysteretic damping during the shaking table tests. Since the retrofit stiffened and repaired the damage to the critical interior columns of the model, the contributions from hysteretic behavior to the "equivalent viscous damping" are significantly reduced. However, the viscous damping is not a suitable model for the energy dissipation and therefore, the equivalent ratios are not used in analysis.

The updated stiffness matrix of the model using the dynamic characteristics of WHNR_B is shown in Table 3-2 along with the corresponding story stiffnesses. It can be observed that the sum of the diagonal terms of the stiffness matrix is increased by about 800% after retrofit. Story stiffness increases of 440%, 1140%, and 860%, respectively for the first, second, and third stories have resulted after retrofit. The different stiffness change of the first story compared to the changes in the second and third stories is due to the discontinuity of the added rebars into the base and lack of prestressing in the lower first story columns. Also note that the stiffness change of the first floor correlates to the change in first mode natural frequency as follows:

$$\frac{f_r}{f_f} = \sqrt{\frac{k_r}{k_f}} \tag{3.1}$$

where f_r = first mode natural frequency from WHNR_B (after retrofit)

f_f = first mode natural frequency from WHN_F (before retrofit)

k_r = first story stiffness from WHNR_B

k_f = first story stiffness from WHN_F

Fig. 3-3 shows the story shear versus inter-story drift histories for WHNR_B. It can be observed that loops occur in these histories mostly due to the equivalent damping present in the structure. The initial stiffnesses for small amplitude displacements are tabulated in Table 3-3 and correspond to increases of about 300%, 600%, and 600%, respectively after retrofit as compared to WHN_F.

At the conclusion of white noise excitation WHNR_B, the table was set down for the day (1/28/92). The next day (1/29/92), the table was again lifted and another white noise excitation, WHNR_C, was performed for identification of the dynamic characteristics of the model. Fig 3-4 shows the smoothed story transfer functions. The natural frequencies, modal shapes, modal participation factors, and equivalent viscous damping factors are calculated and tabulated in Table 3-4. It can be observed that the natural frequencies are reduced by 5.0%, 2.1%, and 0.3%, respectively from the induced white noise shaking table excitation and/or the lowering and lifting of the shaking table. Although it is considered that this reduction is minor. Comparable modal shapes and participation factors can be observed between WHNR_B and WHNR_C. A variation can be observed in comparing the first mode damping factors of WHNR_B and WHNR_C from Table 3-4, which indicates the occurrence of some non-linear cracking behavior in the model due to the white noise excitation.

The updated stiffness matrix and story stiffnesses of the model, using the dynamic characteristics of WHNR_C, is shown in Table 3-4. It can be observed that the sum of the diagonal terms of the stiffness matrix is reduced by 1.6% and a 18.8% story stiffness degradation occurs to the first story due to the movement of the model during the white noise excitation tests and during the lowering and lifting of the shaking table to operating positions.

Fig. 3-5 shows the story shear versus inter-story drift histories for WHNR_C. From Table 3-5, the initial stiffnesses for small amplitude displacements are comparable with the stiffnesses from WHNR_B (Fig. 3-3), but slightly softened.

Therefore it is concluded that the lowering and lifting process and/or the input white noise shaking table excitation inflicts some minor softening to the retrofitted model structure, but is considered insignificant for the strong base motion testing.

TABLE 3-2 Dynamic Properties and Stiffness Matrix before and after Retrofit

	WHN_F (before retrofit)	WHNR_B (after retrofit)
Natural Frequencies (Hz.)	$\mathbf{f}_i = \begin{pmatrix} 1.20 \\ 3.76 \\ 5.27 \end{pmatrix}$	$\mathbf{f}_i = \begin{pmatrix} 2.78 \\ 9.38 \\ 16.75 \end{pmatrix}$
Modal Shapes	$\Phi_{ij} = \begin{pmatrix} 1.00 & -0.86 & -0.46 \\ 0.75 & 0.64 & 1.00 \\ 0.33 & 1.00 & -0.94 \end{pmatrix}$	$\Phi_{ij} = \begin{pmatrix} 1.00 & -0.86 & -0.51 \\ 0.79 & 0.48 & 1.00 \\ 0.42 & 1.00 & -0.89 \end{pmatrix}$
Modal Participation Factors	$\Gamma_i = \begin{pmatrix} 0.43 \\ 0.14 \\ -0.07 \end{pmatrix}$	$\Gamma_i = \begin{pmatrix} 0.44 \\ 0.12 \\ -0.07 \end{pmatrix}$
Damping Ratios (%)	$\xi_i = \begin{pmatrix} 7.0 \\ 2.3 \\ 1.8 \end{pmatrix}$	$\xi_i = \begin{pmatrix} 3.0 \\ 1.9 \\ 1.3 \end{pmatrix}$
Stiffness Matrix (kip/in)	$\mathbf{K}_{ij} = \begin{pmatrix} 23.3 & -24.8 & 0.7 \\ -24.8 & 45.6 & -22.4 \\ 0.7 & -22.4 & 51.0 \end{pmatrix}$	$\mathbf{K}_{ij} = \begin{pmatrix} 205.2 & -238.6 & 71.6 \\ -238.6 & 421.4 & -278.2 \\ 71.6 & -278.2 & 432.7 \end{pmatrix}$
Story Stiffnesses (kip/in)	$\mathbf{k}_i = \begin{pmatrix} 24.8 \\ 22.4 \\ 28.6 \end{pmatrix}$	$\mathbf{k}_i = \begin{pmatrix} 238.6 \\ 278.2 \\ 154.5 \end{pmatrix}$

TABLE 3-3 Low Amplitude Initial Stiffnesses from the Shear versus Inter-Story Drift Histories

Story	WHN_F (kip/in)	WHNR_B (kip/in)
Third	14.3	100.0
Second	14.3	100.0
First	27.8	113.2

TABLE 3-4 Dynamic Properties and Stiffness Matrix of the Retrofitted Structure from WHNR_B and WHNR_C

	WHNR_B	WHNR_C
Natural Frequencies (Hz.)	$\mathbf{f}_i = \begin{pmatrix} 2.78 \\ 9.38 \\ 16.75 \end{pmatrix}$	$\mathbf{f}_i = \begin{pmatrix} 2.64 \\ 9.18 \\ 16.70 \end{pmatrix}$
Modal Shapes	$\Phi_{ij} = \begin{pmatrix} 1.00 & -0.86 & -0.51 \\ 0.79 & 0.48 & 1.00 \\ 0.42 & 1.00 & -0.89 \end{pmatrix}$	$\Phi_{ij} = \begin{pmatrix} 1.00 & -0.86 & -0.49 \\ 0.79 & 0.45 & 1.00 \\ 0.44 & 1.00 & -0.83 \end{pmatrix}$
Modal Participation Factors	$\Gamma_i = \begin{pmatrix} 0.44 \\ 0.12 \\ -0.07 \end{pmatrix}$	$\Gamma_i = \begin{pmatrix} 0.44 \\ 0.11 \\ -0.07 \end{pmatrix}$
Damping Ratios (%)	$\xi_i = \begin{pmatrix} 3.0 \\ 1.9 \\ 1.3 \end{pmatrix}$	$\xi_i = \begin{pmatrix} 4.7 \\ 1.8 \\ 1.6 \end{pmatrix}$
Stiffness Matrix (kip/in)	$\mathbf{K}_{ij} = \begin{pmatrix} 205.2 & -238.6 & 71.6 \\ -238.6 & 421.4 & -278.2 \\ 71.6 & -278.2 & 432.7 \end{pmatrix}$	$\mathbf{K}_{ij} = \begin{pmatrix} 198.9 & -238.2 & 65.2 \\ -238.2 & 438.5 & -279.1 \\ 65.2 & -279.1 & 404.6 \end{pmatrix}$
Story Stiffnesses (kip/in)	$\mathbf{k}_i = \begin{pmatrix} 238.6 \\ 278.2 \\ 154.5 \end{pmatrix}$	$\mathbf{k}_i = \begin{pmatrix} 238.2 \\ 279.1 \\ 125.5 \end{pmatrix}$

TABLE 3-5 Low Amplitude Initial Stiffnesses from the Shear versus Inter-Story Drift Histories

Story	WHNR_B (kip/in)	WHNR_C (kip/in)
Third	100.0	96.8
Second	100.0	96.8
First	113.2	109.1

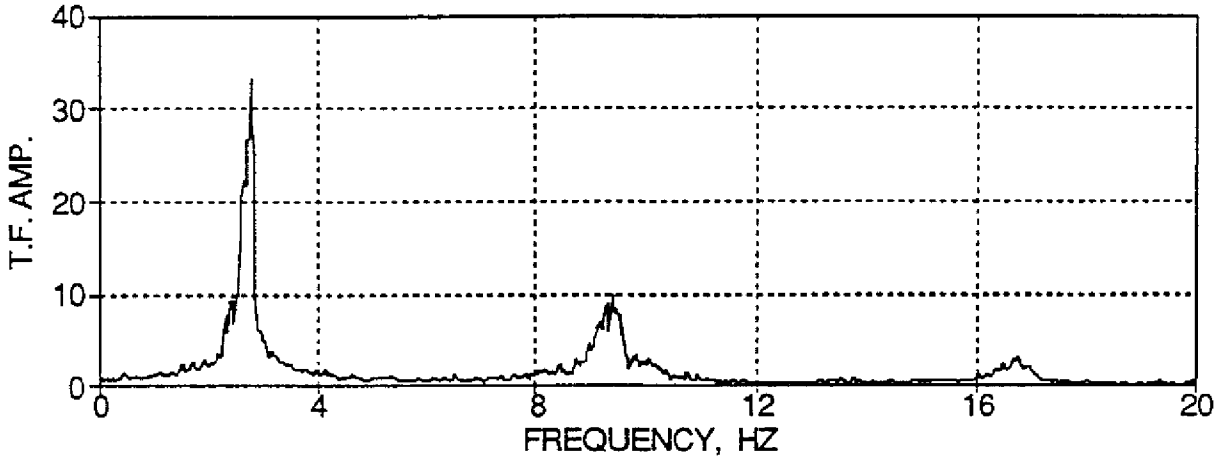

(a) Third Floor

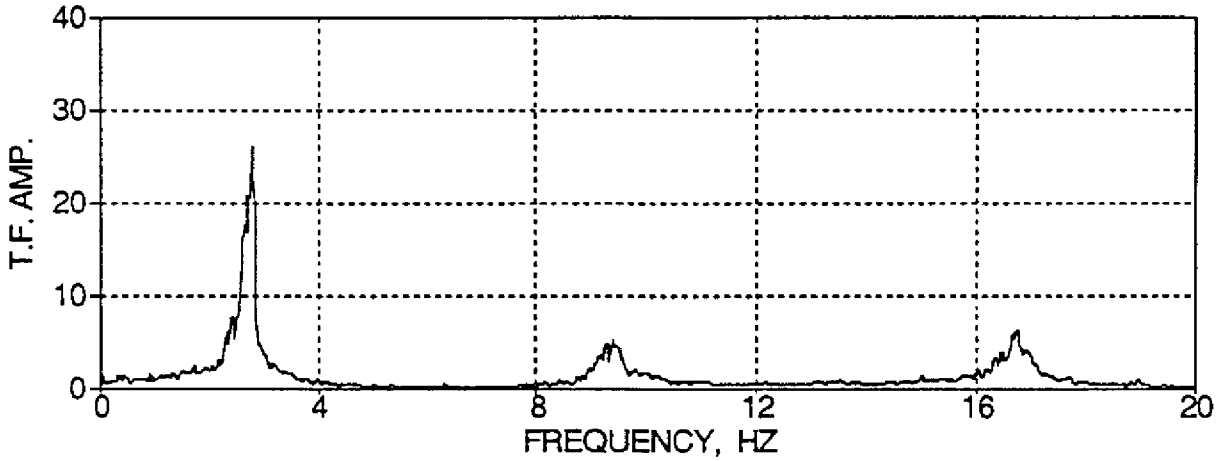

(b) Second Floor

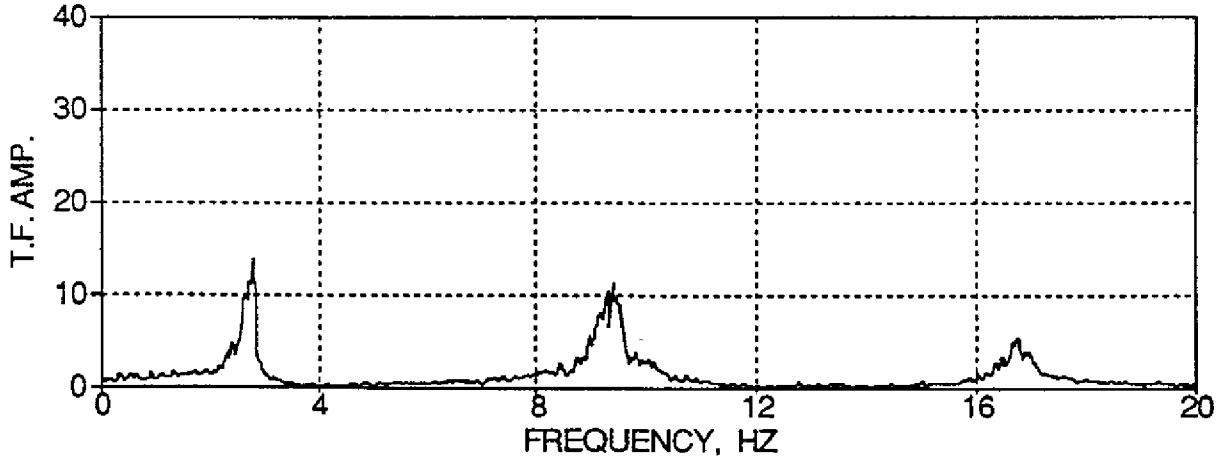

(c) First Floor

FIG. 3-2 Smoothed Transfer Functions from WHNR_B

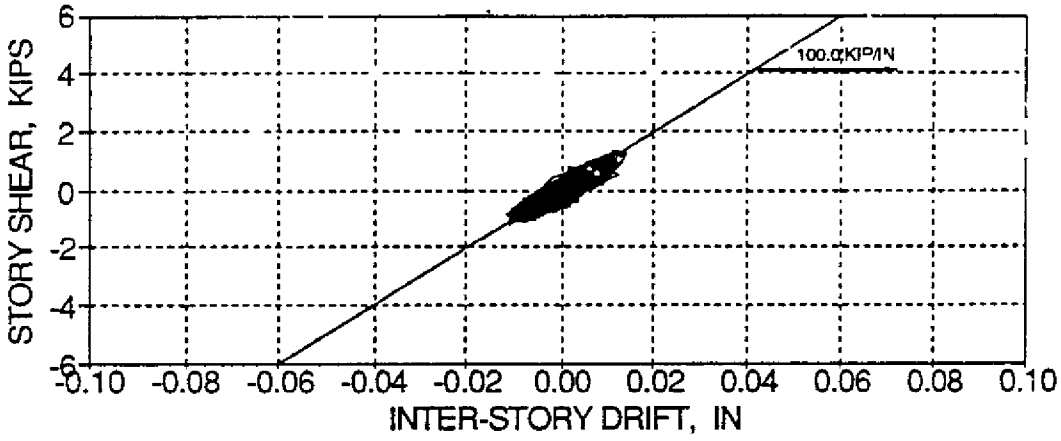

(a) Third Floor

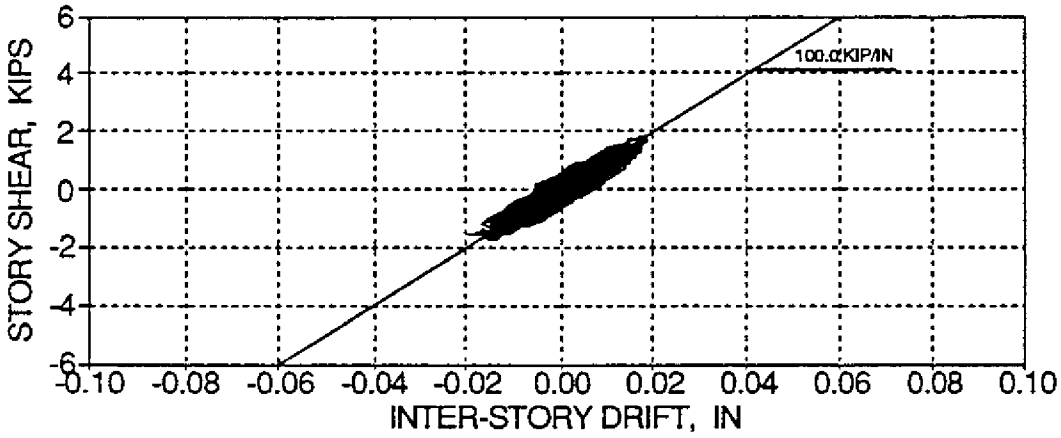

(b) Second Floor

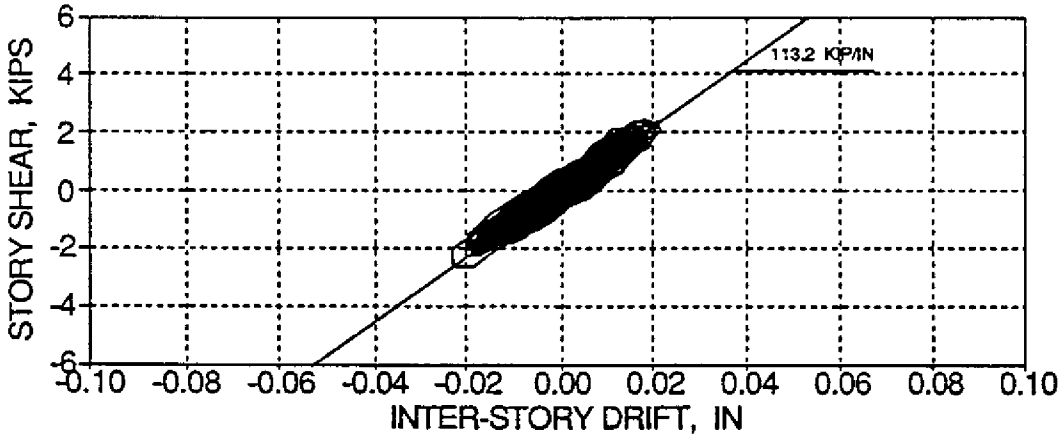

(c) First Floor

FIG. 3-3 Story Shear versus Inter-Story Drift Histories for WHNR_B

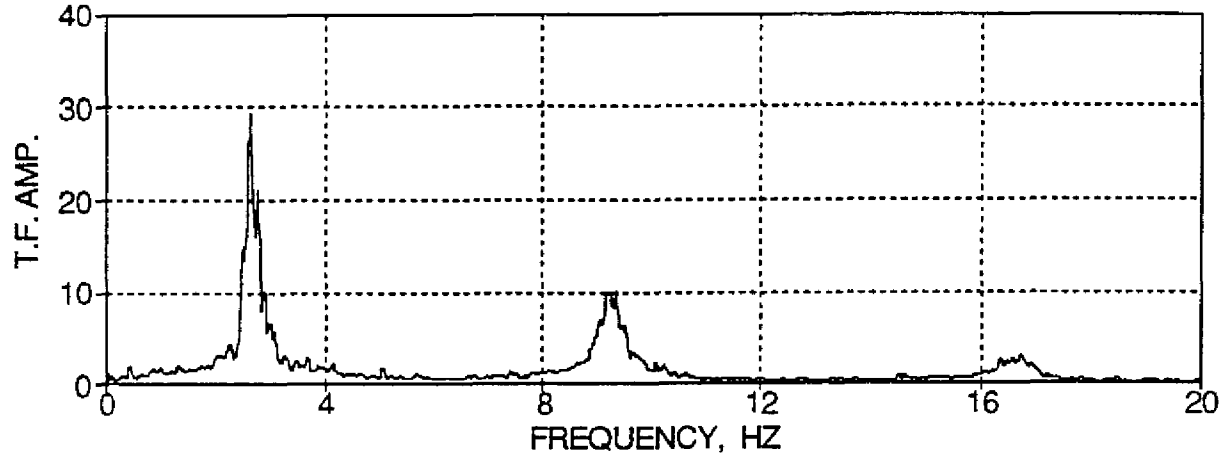

(a) Third Floor

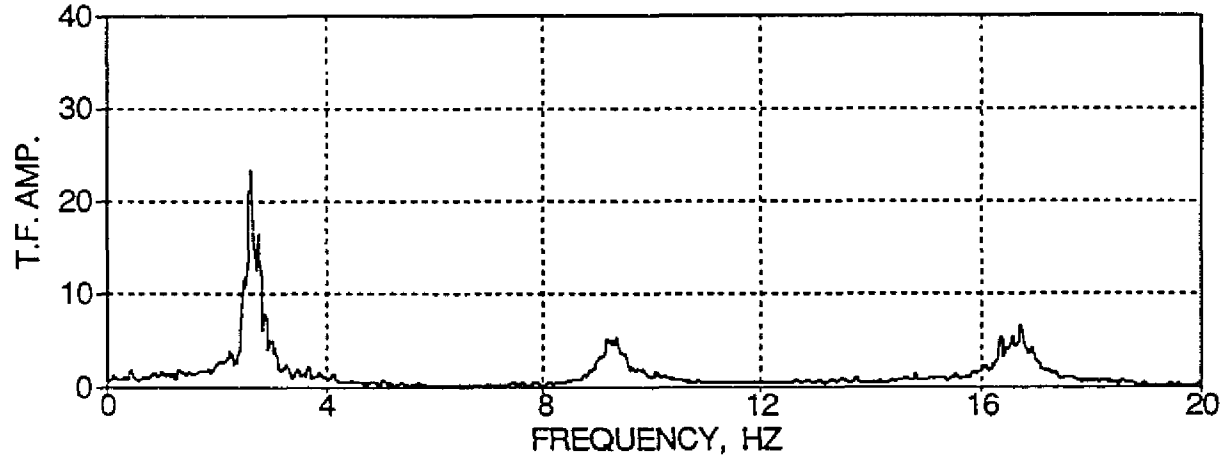

(b) Second Floor

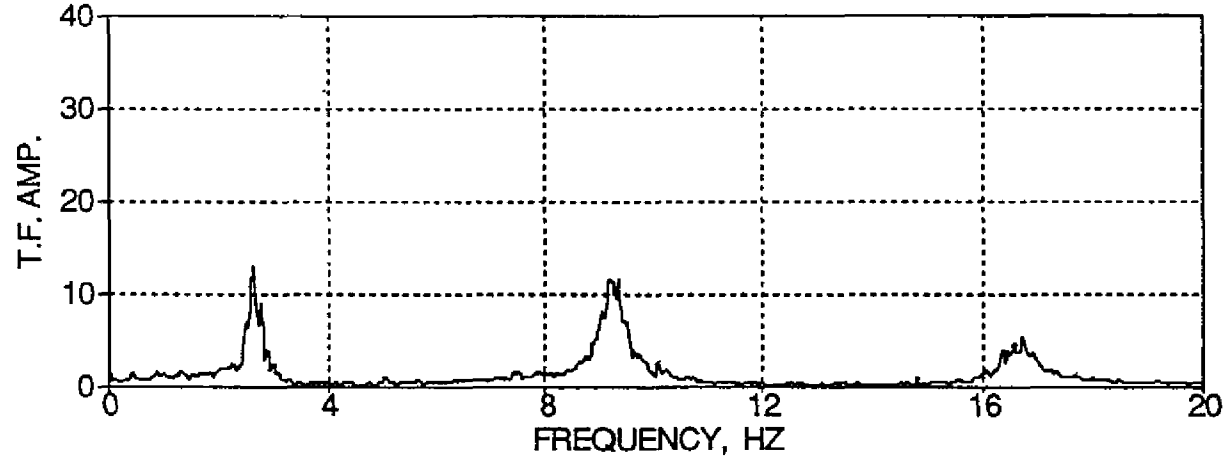

(c) First Floor

FIG. 3-4 Smoothed Transfer Functions from WHNR_C

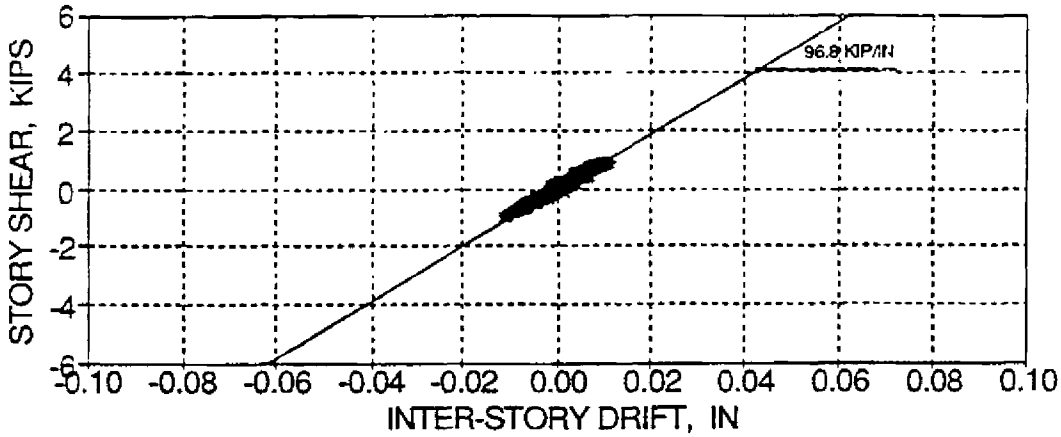

(a) Third Floor

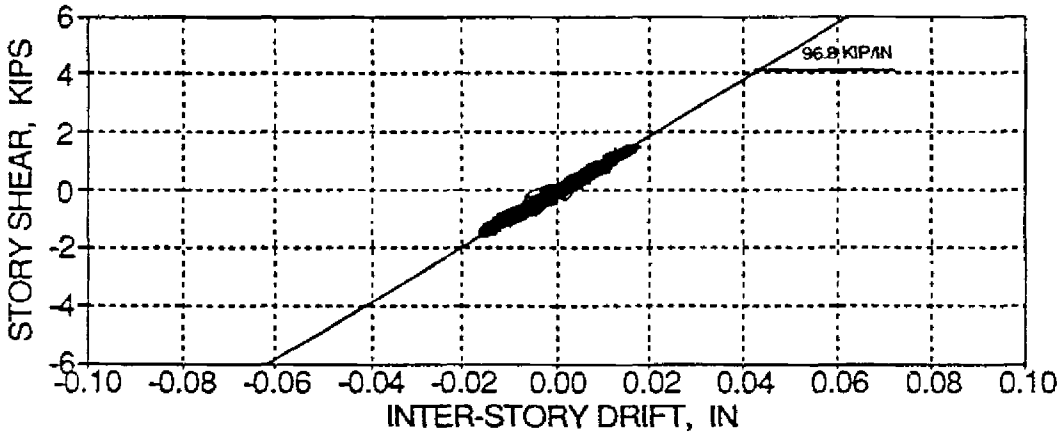

(b) Second Floor

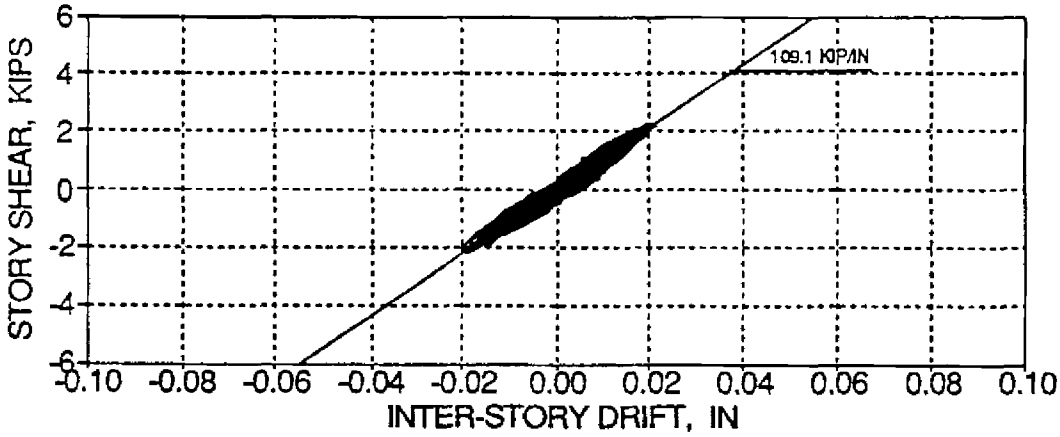

(c) First Floor

FIG. 3-5 Story Shear versus Inter-Story Drift Histories for WHNR_C

3.5 Summary Discussions

The retrofit method selected for the damaged model is the improved concrete jacketing of the interior columns with a weak base retrofit. This retrofit technique: (i) provides satisfactory control of response from seismic forces; (ii) is easy and inexpensive to construct; (iii) requires minimal material that is readily available; and (iv) is a feasible retrofit for the model building.

From the white noise excitation of the retrofitted model, the dynamic properties indicate:

(1) Story stiffness increases of about 440%, 1140%, and 860%, respectively for the first, second, and third floors, as expected. This corresponds to increases in natural frequencies of about 130%, 150%, and 210%, respectively for the first three modes of vibration.

(2) A decrease in equivalent viscous damping from smaller contributions of hysteretic damping after retrofit. This decrease is attributed to the effect of prestressing which ensures the columns behave in an uncracked linear-elastic state.

The testing of the retrofitted model under simulated earthquakes is planned to verify:

(1) A change in formation of the potential collapse mechanism under ultimate load from an undesirable column-sidesway/soft-story mechanism to a more desirable beam-sidesway mechanism.

(2) A reduction of inter-story drifts due to additional stiffening.

(3) A reduction in the expected damage states due to strengthening of the columns.

(4) The use of post-tensioning, to avoid placement of transverse shear steel, leads to a satisfactory structural performance and joint behavior.

(5) Constructability and economical aspects.